Microbial biodegradation and metabolite toxicity of three pyridinium-based cation ionic liquids

Kathryn M. Docherty,*[a] Michelle V. Joyce,[b] Konrad J. Kulacki[c] and Charles F. Kulpa[d]

Received 15th September 2009, Accepted 21st January 2010
First published as an Advance Article on the web 25th February 2010
DOI: 10.1039/b919154b

Merging the disciplines of green chemistry, ecotoxicology and ecology to develop environmentally-friendly industrial chemicals represents a significant collaborative challenge. This challenge can be met by extending already-informative standard toxicity and biodegradability assays to include further information about the potential persistence and biotransformation of pollutants in the environment. Development of ionic liquids (ILs) provides an ideal and proactive test system to determine several levels of environmental impact using academically interesting and industrially relevant green chemical prototypes. In this study, we investigated the biodegradability of three ILs, 1-butyl-3-methylpyridinium bromide, 1-hexyl-3-methylpyridinium bromide and 1-octyl-3-methylpyridinium bromide, by activated sludge microbial communities. We determined that all three ILs could be fully mineralized, but that only the octyl-substituted cation could be classified as "readily biodegradable". We directly examined biodegradation products of the ILs using reverse-phase high performance liquid chromatography/mass spectrometry and MS/MS methods, and identified several unique preliminary degradation products. Finally, we determined that IL-biodegradation products were less toxic than the initial compound to a standard aquatic test organism, *Daphnia magna*, suggesting that biodegradation in an aquatic environment would decrease toxicity hazards associated with the initial compound. This study provides further information about pyridinium IL-biodegradation and guidelines to structure future IL design and research.

Introduction

It is generally acknowledged that many of our current technologies are unsustainable because their operation is incompatible with the long-term well-being of organisms and the environment.[1] Green chemistry, as a discipline, strives to surpass the present quality of life achieved by chemical advances, while using products and processes that are benign to human health and the environment.[2] Specifically, this means using starting materials and processes that have practical chemical properties (*e.g.*, low explosivity, flammability, volatility and corrosivity), as well as low acute and chronic toxicity, carcinogenicity and mutagenicity, and do not persist or bioaccumulate in the environment. The field of green chemistry operates under "Twelve Principles", two of which inevitably and inseparably link it to the field of ecotoxicology: Principle 4 – design chemicals for reduced toxicity while maintaining efficacy and function; and Principle 10 – design chemicals for degradation which will break down into innocuous products that do not persist in the environment.[2]

Extending the bridge between the fields of green chemical engineering and (eco)toxicology has called for both an admirable amount of collaboration between investigators of both disciplines,[1,3,4] as well as a marked reassessment of the effectiveness and ecosystem-applicability of traditional ecotoxicological studies.[5–8] General consensus is that in order to perform a thorough ecological risk assessment (and therefore, fully classify a chemical as "green"), it is important to extend our toxicological analyses beyond the traditional single-species experiments. While this means extending studies to include multiple trophic levels, abiotic interactions and general "chemical stress ecology",[5] it also suggests that testing and subsequent design for nontoxic biodegradation is a crucial part of proactive green chemical design.

While it may be impossible to predict the effects a chemical may have upon an entire ecosystem, it is important to address how biodegradation of a chemical compound may affect the accuracy of risk assessment model predictions based on standard toxicity tests and chemical life cycle assessments. At least partial chemical transformation (if not full degradation) of a chemical compound is likely once a chemical is released into a wastewater treatment plant or directly into the environment itself. Whether through a variety of possible microbial bioactivities, photodegradation and other abiotic interactions, or chemical reactions in the tissues of exposed organisms themselves, chemical structures of pollutants are bound to change.[9] These

[a]*Center for Ecology and Evolutionary Biology, 5289 University of Oregon, 307 Pacific Hall, Eugene, OR, 97405, USA. E-mail: kathrynd@uoregon.edu; Fax: 541-346-2364; Tel: 541-346-5279*
[b]*Department of Chemistry and Biochemistry, University of Notre Dame, Notre Dame, IN, 46556, USA. E-mail: mjoyce@nd.edu*
[c]*Ecology, Evolution & Marine Biology, University of California, Santa Barbara, Santa Barbara, CA, 93106-9610, USA. E-mail: kulacki@lifesci.ucsb.edu*
[d]*Department of Biological Sciences, University of Notre Dame, Notre Dame, IN, 46556, USA. E-mail: kulpa.1@nd.edu*

changes often result in a structure that is less hazardous than the original pollutant and that can easily be converted into nontoxic biomass and CO_2.[9,10] However, sometimes chemicals are degraded into structures that are more toxic, persistent or transportable, and therefore more harmful, than the initial compound (*e.g.*, polybrominated diphenyl ethers (PBDEs) are converted to more-toxic debromination products;[11] polycyclic aromatic hydrocarbons (PAHs) are oxidized to epoxides which can covalently bind to DNA and result in mutations[9,12]). Therefore, it is imperative to investigate structures and toxicities of possible biodegradation products, as well as the impact those products may have beyond the parent chemical, particularly when designing new chemicals that have a wide range of applicability and inevitable environmental release.

Room-temperature ionic liquids (ILs) provide an ideal test system for proactive risk-assessment investigation. Ionic liquids are a class of salts that are liquid at room temperature, and have become a major focus of proactive collaborative research between the fields of green chemical engineering and (eco)toxicology because of their desirable chemical properties, broad industrial applicability, and potential for academic study. Ionic liquids combine a bulky organic cation, which can be substituted with multiple functional groups, with a small, often halogenated, anion. Given the numerous combinations of cations and anions, ILs can be generated to serve a wide variety of applications. For example, imidazolium and pyridinium-cation based ILs have been academically studied as electrolytes,[13] in acylation, Friedel–Crafts, Diels–Alder, Heck and redox reactions [e.g. 14–19] as mobile phase additives for reverse-phase high-performance liquid chromatography (RP-HPLC),[20] as well as many other applications. Several industrial applications involving ILs are in the early or pre-commercial stages. BASF has researched a commercial extractive-distillation and chlorination processes using ILs.[e.g. 21,22] Degussa (Germany) is interested in ILs for a variety of processes, including antifoaming and dispersing agents and emulsifiers.[21] The French Petroleum Institute has commercialized the use of ILs as solvents involved in butane dimerization to octane.[22]

Given this broad range of applicability and industrial interest, many studies have examined the toxicity of ILs prior to their release into the environment. Tests that investigate toxicity to aquatic organisms are of particular interest because ILs are generally water-soluble, and therefore aquatic ecosystems are likely to receive and transport ILs that are released into the environment. A chemical life cycle assessment of the IL 1-butyl-3-methylimidazolium tetrafluoroborate has shown that it is potentially more efficient and recyclable than traditional solvents.[22] However, when released into the environment, this class of IL could have a significant impact on both aquatic and terrestrial environments, water quality, and human health.[22] As recently reviewed by Kulacki *et al.*[4] and emphasized by Stolte *et al.*,[23] ILs (regardless of the cation identity) follow the general trend of increasing toxicity to aquatic test organisms directly correlated with increases in hydrophobicity, which is strongly related to the length of the substituted alkyl chain. While unrelated to mutagenicity,[24] changes in alkyl chain length are also related to sub-lethal fitness and food web interaction patterns such as aquatic organism grazing and periphyton production[25–27] and filter feeding.[28]

Interestingly, the reverse trend is true for biodegradability – the longer the substituted alkyl chain, the more easily the compound can be broken down by activated sludge microbial communities.[29–31] Several studies have shown that imidazolium-[31–33] and quaternary ammonium-based[34] ILs tend to resist biodegradation, thus reducing their potential environmental safety. Recent studies have shown that ILs containing 1-alkyl-3-methylpyridinium cations can be classified as "readily biodegradable" by standard tests.[29,31,35,36,37] Previous studies suggest that the type of ring substitution (*i.e.* different alkyl chain lengths[29,31] or alkyl *vs.* ester group[35,37]) can serve as a useful metric for determining IL biodegradability from chemical structure, while the number of alkyl substitutions around the ring may be less informative.[37,38] Additionally, the identity of the anion is also strongly related to pyridinium biodegradability (*i.e.* pyridiniums with octylsulfate anions are more biodegradable than those with halide anions.[37]) While past studies indicate that pyridinium cations might be "greener" structures for future IL-design, few studies have examined pyridinium-IL biodegradation products[31,36] or the potential toxicity of these products.

In this study, we re-examine the biodegradability of three pyridinium-IL compounds: 1-butyl-3-methylpyridinium bromide (bmpyrBr), 1-hexyl-3-methylpyridinium bromide (hmpyrBr) and 1-octyl-3-methylpyridinium bromide (ompyrBr), using a standard biodegradability assay. The structures for these ILs are presented in Fig. 1. Our results agree that bmpyrBr can be fully biodegraded (as previously shown by Pham *et al.*[36]). We also show, as per our previous results, that hmpyrBr

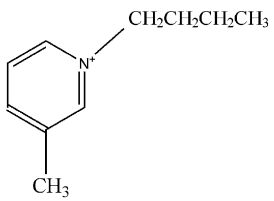

1-butyl-3-methylpyridinium cation (bmpyr)

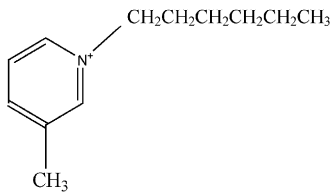

1-hexyl-3-methylpyridinium cation (hmpyr)

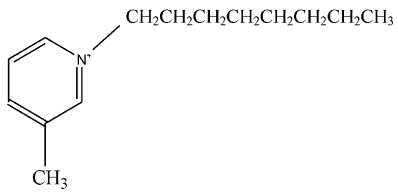

1-octyl-3-methylpyridinium cation (ompyr)

Fig. 1 Chemical structures for 3 test compounds: 1-butyl-3-methylpyridinium bromide, 1-hexyl-3-methylpyridinium bromide and 1-octyl-3-methylpyridinium bromide.

and ompyrBr can be fully biodegraded.[29] However, of the three ILs tested, only ompyrBr can be classified as "readily biodegradable" according to standard test methods. To further aid in prediction of environmental impact and fate of ILs, we examine the degradation products of each of these ILs using direct chemical analyses throughout the biodegradation process. We indicate that unique metabolic products were formed during the degradation of all three ILs, suggesting that several metabolic degradation pathways may be possible for pyridinium-cation ILs. Finally, we determine that the biodegradation products of these three ILs are significantly less toxic to an aquatic test organism after cleavage of the pyridinium ring is achieved. These data provide us with further evidence that pyridinium-based ILs may be rendered environmentally benign to aquatic systems through biodegradation by microorganisms. This study is meant to extend standard biodegradability and toxicity tests to aid in green chemical design and waste management decision-making.

Results and discussion

Recent interest in combining green chemical design with proactive environmental risk assessment has identified many deficiencies in simply using standard toxicity and biodegradability tests to determine whether a chemical is a potential environmental hazard. While useful starting points, standard tests alone provide little information about the transformation and fate of a chemical once it is released into the environment. In this study, we have extended standard biodegradability tests to include direct chemical analyses of biodegradation products as well as an assessment of the toxicity of those products.

Biodegradability by activated sludge microbial communities

Biodegradation, as measured by DOC concentration and absorbance at 265 nm, was analyzed until DOC concentrations reached an average of <5 mg C L^{-1} for the three replicates, indicating full mineralization of the IL (Fig. 2A and 2B). All three ILs exhibited a significant DOC concentration decrease throughout the incubation time period (rmANOVA $p < 0.0039$) as well as a decrease in maximum absorbance at 265 nm (rmANOVA $p < 0.031$). For bmpyrBr and hmpyrBr, full degradation took 41 days, while for ompyrBr it took only 26 days. There were no significant decreases in DOC concentrations of the abiotic controls, indicating that chemical degradation was due to the presence of the microbial activated sludge community (not shown). To determine when microbial biodegradation of the ILs began, we compared experimental sludge-inoculated treatments to the abiotic controls through time. For bmpyrBr, we observed the first significant decrease in DOC concentration on day 28 ($p = 0.003$) and the first significant decrease in maximum absorbance at 265 nm on day 29 ($p = 0.013$). In the hmpyrBr tests, these decreases were observed on day 34 for DOC concentration ($p = 0.044$) and day 35 for absorbance at 265 nm ($p = 0.059$, marginally significant). Finally, for the ompyrBr test, significant decreases occurred on day 18 for DOC concentration ($p = 0.051$, marginally significant) and on day 21 for absorbance at 265 nm ($p = 0.011$). There is agreement between the first day of significant decrease in DOC concentration and the first day of significant decrease in maximum absorbance at 265 nm in all three tests (Fig. 2A and 2B). This indicates that the limiting step to full biodegradation with all three ILs is cleavage of the pyridinium ring. Once the ring has been opened, mineralization occurs rapidly within a 10-day window.

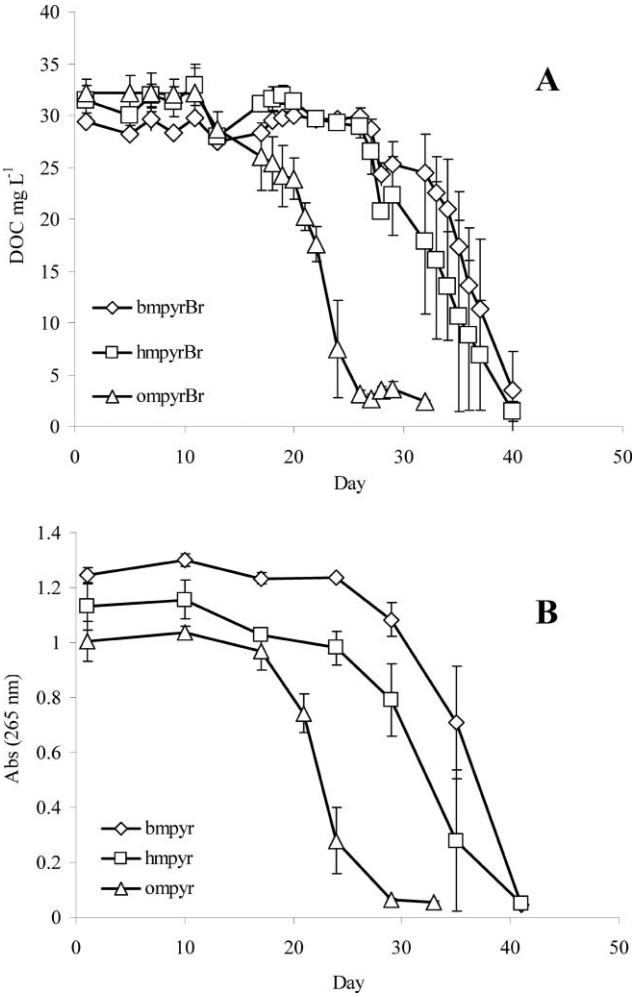

Fig. 2 Whole-community biodegradation experiment DOC concentrations (mg C L^{-1}) (A) and absorbance at 265 nm (B) through the 41-day incubation period. Error bars represent ±1 standard deviation ($n = 3$).

Results from the OECD DOC-Die Away test indicate that ompyrBr is the only one of the three ILs tested that falls within the parameters of "readily biodegradable" as outlined in the OECD protocol. "Readily biodegradable" compounds are defined as those that exhibit a loss of 10% DOC, increasing to a loss of at least 60% DOC within a 10-day window, in a total 28-day long incubation period.[39] In the ompyrBr biodegradation test, a 10% decrease in DOC concentration compared to the control began on day 18, and within 10 days, the concentration decreased by 60% (Fig. 2A). Additionally, DOC decreased by 92% by the final day of the experiment (day 33). While bmpyrBr and hmpyrBr DOC concentrations both decreased after 41 days (88% and 95%, respectively), these ILs cannot be classified as "readily biodegradable" because they did not biodegrade within a 28-day period.

These results confirm prior analyses that show a correlation between the length of the substituted alkyl chain on the pyridinium ring and whole-compound biodegradability.[29–31] Previous results from our group have shown that bmpyrBr could not be mineralized after 43 days using similar methods and microbial communities obtained from the same wastewater treatment plant that was used in this study.[29] ^{1}H-NMR results from the final day indicated that the bmpyr cation was still intact, suggesting resistance to degradation.[29] The results here indicate that bmpyrBr can be fully biodegraded, though it still cannot be considered "readily biodegradable" by OECD standards. This is contrary to the results found by Pham *et al.*[36] Since similar concentrations were used in the current study as in our previous examination of bmpyrBr biodegradability, it is unlikely that bmpyrBr toxicity significantly impacted the active microbial consortium, as suggested by Pham *et al.*[36] Instead, it is more likely that a particular activated sludge sample may vary in microbial community composition, both by wastewater treatment plant as well as seasonally within the same plant. This may impact both the efficiency and mechanism of biodegradation. Spatial and temporal variation in wastewater treatment plants has been shown to affect degradation capacity.[40,41] Additionally, very specific changes in microbial community composition may alter degradation efficiency or even ability.[42] Incorporating several treatment plant samples into standard biodegradability assays may provide useful information about what communities are necessary to degrade a particular chemical of interest. Proactively assessing communities capable of biodegradation for newly engineered chemicals using molecular microbial ecology techniques, as well as determining whether a chemical is degraded by a cultivatable isolate or a microbial consortium, could provide valuable means for pollution prevention as well as parameters to models predicting environmental fate.

Biodegradability using HPLC/mass spectrometry

To investigate IL-metabolite structures, we removed and concentrated samples on days 1, 10, 17, 24, 29, 35 and 41 from the bmpyr and hmpyr experimental treatments and on days 1, 10, 17, 21, 24, 29 and 33 from the ompyr treatment for further examination using HPLC/MS. Different chemical structures can be separated based on their hydrophobicities on a reverse-phase HPLC column and then by their mass-to-charge ratios (m/z value) in the mass spectrometer. Peaks with different retention times corresponding to the same m/z value most likely indicate structural-isomer variations. For each IL, the intact molecule, M, consists of the pyridinium cation and bromide anion. Thus, bmpyrBr is signified by M_B, hmpyrBr by M_H and ompyrBr by M_O. However, dissolution in water allowed us to monitor the cation without its counter anion. Thus, the detected intact IL base peaks were m/z 150 for $[M_B - Br]^+$ at 5.5 min for bmpyr, m/z 178 for $[M_H - Br]^+$ at 8.3 min for hmpyr, and m/z 206 for $[M_O - Br]^+$ at 10.3 min for ompyr. The original RP-HPLC/MS chromatograms (not shown) provide estimate of the concentration of initial test compound to metabolite compound concentration (Fig. 3). It should be noted that different acetonitrile–aqueous gradients on the LC column were used to optimize each IL separation, making retention times among the three ILs not comparable.

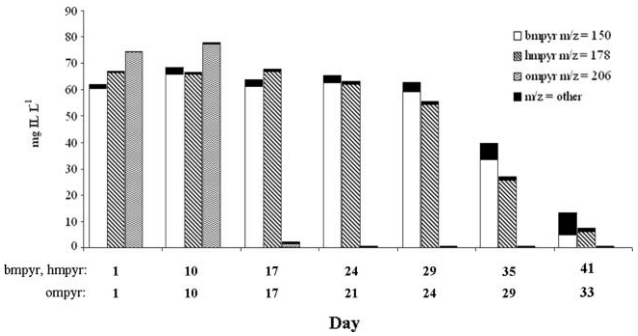

Fig. 3 Concentration of IL (mg L^{-1}) determined by HPLC-MS, of one replicate of each of the three pyridinium ILs, and the sum of the detectable pyridinium-based biodegradation products for each time point during the 41-day whole-community biodegradation experiment. Note that incubation time (x-axis) is different for ompyrBr.

As suggested by the DOC concentration and absorbance data (Fig. 2A and 2B), once the pyridinium ring is opened, biodegradation occurs quite rapidly, so the products after ring cleavage are likely aliphatic and very labile to microorganisms. This result is emphasized by comparison of the peak intensity for each initial structure to the summed peak intensities of the metabolite structures of an IL using RP-HPLC/MS through time (Fig. 3). The base peak (or that which has the highest intensity in a spectrum) in each MS spectrum in this study always corresponds to the intact IL structure, with the exception of the day 41 bmpyr degradation data point. These results suggest that the rate-limiting step for 1-alkyl-3-methylpyridinium IL degradation involves the first microbial action upon the chemical structure and that few recalcitrant metabolites are produced (Fig. 3). Most metabolites do not contain an aromatic ring or are incorporated into microbial biomass or released as CO_2 or another gas, and therefore were not detectable by the methods used in this study.

Metabolite structure assessed by RP-HPLC/MS and MS/MS

As in previous studies[31,36] only biodegradation products that contained a pyridinium ring could be detected above the sample background using our LC/MS method, therefore full biodegradation pathway elucidation was not possible. This is due to a combination of factors, including a high amount of other microbe-associated carbon molecules present in the samples, as well as low concentrations of a diverse array of possible biodegradation products compared to those products with the ring intact. These detection limitations suggest that further analysis of IL biodegradation pathways will need to include radio- and/or stable isotope-labeled ILs, as well as higher initial concentrations, to enable separation and detection above background. Unfortunately, it is currently cost-prohibitive to perform labeled-isotope experiments, since most ILs are synthesized in academic labs.

Despite these detection limitations, the LC/MS method we employed did yield peaks other than the IL cation that were detected in the MS spectra of the ILs at different time points (shown as Potential Metabolite Structures in Fig. 4, 5 and 6). We used MS/MS (also referred to as tandem MS) to further assess these peaks which were detected by MS and to determine if they corresponded to structures relating to the theoretical starting

points of biodegradation. This method utilizes collision-induced dissociation (CID) to fragment a selected *m/z* value, (the parent ion, in this case, a particular IL biodegradation product) using argon gas. Through CID the parent ion is fragmented into smaller ions, or daughter ions, that are analyzed to gain further insight into the structure of the parent ion from which they originate. In most cases, the pyridinium ring was highly resistant to fragmentation by argon gas, even at collision energies exceeding 100 kV, which is higher than those used in most MS/MS protocols. This is due to the fact that these pyridinium structures are both incredibly small and stable for traditional fragmentation. Additionally, due to the low concentration of the degradation products in some samples, particularly in the latter time points, the low signal-to-noise ratio of the daughter ions in the MS/MS spectrum against the background of the sample also deterred identification. Despite these limitations we were able to obtain some information about the structure of the initial pyridinium-based degradation products. Here we address each set of metabolites related to each of the three ILs separately:

Initial compound bmpyr [M_B – Br^-], *m/z* 150 (Fig. 4). The MS spectrum (not shown) of [M_B – Br] on Day 41 indicated three major degradation products: *m/z* 148 (retention time 5.08 min), *m/z* 166 (retention times 4.03, 9.99 and 15.09 min) and *m/z* 164 (retention time 7.55 min). The sum of these products for each time point is shown in black as "*m/z* = other" in Fig. 3. In the case of bmpyr, as well as hmpyr and ompyr, MS/MS experiments were performed on the degradation products (Panels B, C and D of Fig. 4, 5 and 6, respectively), as well as on the intact IL (Panel A of Fig. 4, 5 and 6 respectively), to aid in structural elucidation. The MS/MS spectrum for the bmpyr parent ion *m/z* 150 (Fig. 4, Panel A) yielded the following daughter ions: *m/z* 94.2 corresponding to 1-methylpyridine; *m/z* 57 corresponding to a butyl group (the alkyl side chain of the intact IL); *m/z* 43 indicating a propyl group (partial degradation of the side chain), and *m/z* 29 indicating an ethyl group (further degradation of the side chain)

The MS/MS spectrum for the parent ion *m/z* 148 (Fig. 4, Panel B) indicates that the metabolite structure is [M_B – Br – 2H]$^+$, where two hydrogen atoms have been removed from the butyl group to reduce the total mass. This assignment is due to the fact that the 1-methylpyridine group is intact (daughter ion *m/z* 94 is present), but the butyl group has been reduced by a mass of two atoms to yield a daughter ion *m/z* 55. We were unable to identify daughter ion *m/z* 132 in this spectrum, but suggest this structure may correspond to 1,3-dimethylpyridine or a structure where the 1-butyl group has been partially degraded either by rearrangement or removal of three carbon atoms.

The MS/MS spectrum of the parent ion *m/z* 166 (Fig. 4, Panel D) suggests that the metabolite structure is a 1-butyl-3-methylpyridine molecule with a single hydroxyl group substituted at one of the ring-carbon positions, though we are not able to determine the position of the hydroxyl group. It should be noted that in our MS/MS figures, a ▼ symbol indicates the potential position of a single hydroxyl group, as opposed to the presence of several hydroxyl groups. Daughter ion *m/z* 110 indicates a hydroxylated 3-methylpyridine structure and daughter ion *m/z* 57 indicates an intact butyl group.

We were unable to conclusively identify the [M_B – Br] metabolite corresponding to parent ion *m/z* 164 due to a low signal/noise (S/N) of the daughter ions in the MS/MS spectrum (Fig. 4, Panel C). Based on the *m/z* value determined by MS alone, we suggest that this structure corresponds to a combination of the two variants seen with parent ions *m/z* 148 (Fig. 4, Panel B) and *m/z* 166 (Fig. 4, Panel D), where the butyl chain is reduced by a mass of 2 hydrogen atoms, and the pyridinium ring is substituted with one hydroxyl group (Fig. 4, Panel C).

Initial compound hmpyr [M_H – Br^-], *m/z* 178 (Fig. 5). The MS spectra (not shown) of [M_H – Br^-], on Days 29 and 35 indicated three major degradation products: *m/z* 176 (retention times 4.17 and 7.40 min), *m/z* 192 (retention times 2.72 and 10.4 min) and *m/z* 194 (retention times 4.3 and 5.88 min). The sum of these products for each time point is shown in black as "*m/z* = other" in Fig. 3. The MS/MS spectrum for the hmpyr parent ion *m/z* 178 (Fig. 4, Panel A) yielded the following daughter ions: *m/z* 94.2 corresponding to 1-methylpyridine; *m/z* 85 indicating a hexyl group; *m/z* 57 from a butyl group; *m/z* 43 indicating a propyl group.

The MS/MS spectrum of the biodegradation product parent ion *m/z* 176 (Fig. 5, Panel B), indicates that the metabolite structure contains a partially degraded side chain. While we can not definitively identify the structure, daughter ion *m/z* 94 indicates that 3-methylpyridine remains intact and the presence of the daughter ion *m/z* 132 suggests side-chain degradation by three carbon atoms and side chain rearrangement.

The MS/MS spectrum of the biodegradation product parent ion *m/z* 192 (Fig. 5, Panel C) suggests the identification of the metabolite structure as 1-hexyl-3-methylpyridine with a hydroxyl group substituted on the hexyl side chain. The presence of both intact 3-methylpyridine (daughter ion *m/z* 94) and a re-arranged hydroxyl-substituted hexyl side chain (daughter ion *m/z* 99.1) are suggestive of this metabolite structure.

Finally, the MS/MS spectrum of the parent ion *m/z* 194 (Fig. 5, Panel D) indicates that this metabolite is 1-hexyl-3-methylpyridine plus a single hydroxyl group substituted on a ring position. The presence of daughter ions in this spectrum with *m/z* 43 and *m/z* 85 indicate that the hexyl chain is intact and unsubstituted. The presence of daughter ion *m/z* 110 indicates a 3-methylpyridine structure that has been substituted with a hydroxyl group on the ring, though the exact position cannot be identified. We were unable to identify the daughter ion *m/z* 153, but suggest that this may correspond again to 1-hexyl-3-methylpyridine in which rearrangement or degradation of the hexyl side chain has occurred.

It should be noted that each of the three major degradation products of hmpyr were found in two peaks in the LC/MS total ion current trace eluting at different times. In each case, the two peaks of the same *m/z* value but different retention time indicate structural isomers of the compound. Therefore the unsaturation and hydroxylation occurred at different positions on the compound to yield metabolite structures with different hydrophobicities.

Initial compound ompyr [M_O – Br^-], *m/z* 206 (Fig. 6). The MS spectra (not shown) of [M_O – Br^-], on Days 17 and 29

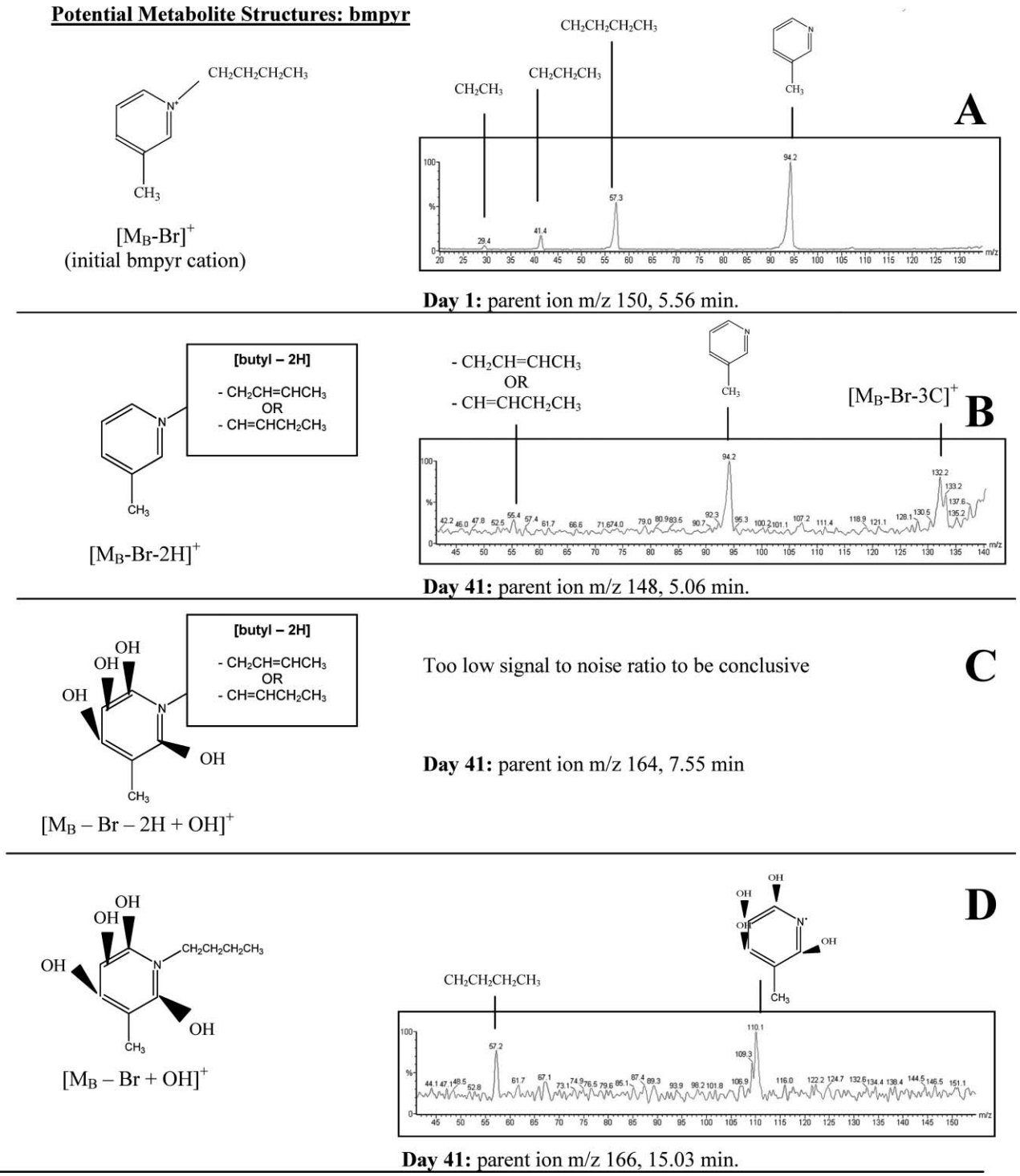

Fig. 4 MS/MS results for initial bmpyr ($[M_B – Br]^+$) parent ion m/z 150 (Panel A), and biodegradation metabolite parent ions m/z 148 (Panel B), m/z 164 (Panel C) and m/z 166 (Panel D). Each MS/MS spectrum represents a scan of a single replicate on the indicated experiment days and daughter ion fractionation products are identified above each spectrum to indicate how the parent ion was identified. Parent ions for the initial bmpyr cation and the three potential metabolite structures are presented to the left of each corresponding spectrum. ▼ symbolizes the potential positions for a single hydroxyl substitution around the ring, not the presence of 4 hydroxyl groups.

indicated three major degradation products: m/z 204 (retention time 7.68 min), m/z 222 (retention time 2.60 min) and m/z 224 (retention time 1.86 min) The sum of these products over time is shown in black as "m/z = other" in Fig. 3. The MS/MS spectrum of the initial $[M_O – Br]$ parent ion m/z 206 (Fig. 6, Panel A) yielded daughter ion m/z 120 corresponding to the intact ompyr cation with the loss of six carbon atoms from the side chain; m/z 107 presumably from the ompyr cation with the loss of seven carbon atoms from the side chain; m/z 94.2 indicating 3-methylpyridine; m/z 71 corresponding to a pentyl

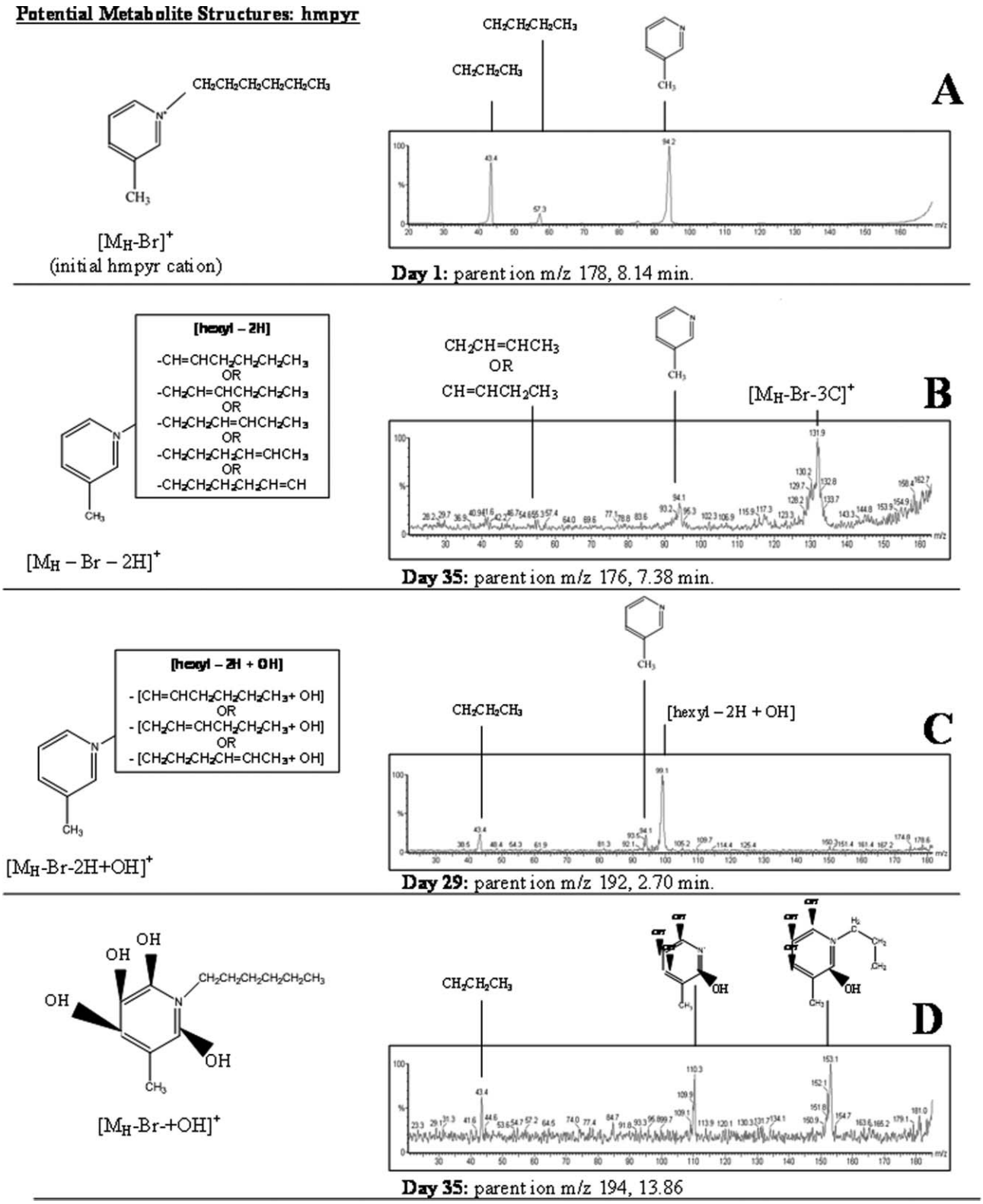

Fig. 5 MS/MS results for initial hmpyr ($[M_H - Br]^+$) parent ion *m/z* 178 (Panel A), and biodegradation metabolite parent ions *m/z* 176 (Panel B), *m/z* 192 (Panel C) and *m/z* 194 (Panel D). Each MS/MS spectrum represents a scan of a single replicate on the indicated experiment days and daughter ion fractionation products are identified above each spectrum to indicate how the parent ion was identified. Parent ions for the initial hmpyr cation and the three potential metabolite structures are presented to the left of each corresponding spectrum. ▼ symbolizes the potential positions for a single hydroxyl substitution around the ring, not the presence of 4 hydroxyl groups.

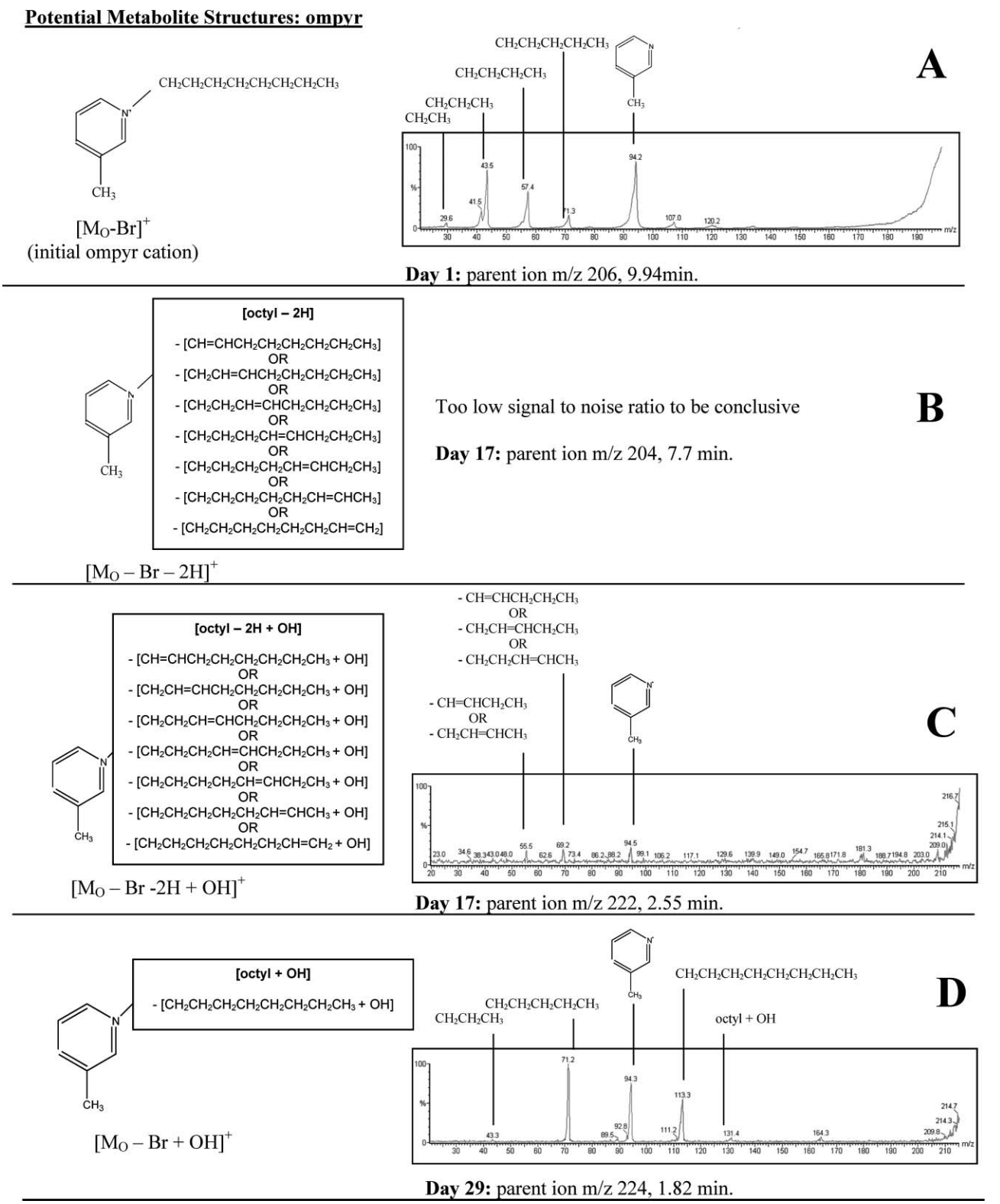

Fig. 6 MS/MS results for initial ompyr ($[M_O - Br]^+$) parent ion *m/z* 206 (Panel A), and biodegradation metabolite parent ions *m/z* 204 (Panel B), *m/z* 222 (Panel C) and *m/z* 224 (Panel D). Each MS/MS spectrum represents a scan of a single replicate on the indicated experiment days and daughter ion fractionation products are identified above each spectrum to indicate how the parent ion was identified. Parent ions for the initial ompyr cation and the three potential metabolite structures are presented to the left of each corresponding spectrum. ▼ symbolizes the potential positions for a single hydroxyl substitution around the ring, not the presence of 4 hydroxyl groups.

group; m/z 57 from a butyl group; and m/z 43 from a propyl group.

We were unable to conclusively identify metabolite biodegradation product for the parent ion m/z 204 from the MS/MS spectrum, but the structure likely corresponds to the ompyr cation with the loss of two hydrogen atoms from the octyl group (Fig. 6, Panel B).

The MS/MS spectrum of the parent ion m/z 222 suggests that the metabolite structure is the ompyr cation substituted with one hydroxyl group on the side chain as well as a loss of two hydrogen atoms from the side chain (Fig. 6, Panel C). Evidence for this structure is provided by the presence of daughter ion m/z 94 from intact 3-methylpyridine, as well as daughter ion m/z 69 as the pentyl with the loss of two hydrogen atoms, and daughter ion m/z 55 as a butyl with the loss of two hydrogen atoms.

Similarly, the MS/MS spectrum of the parent ion m/z 224 suggests that the metabolite structure is the ompyr cation substituted with one hydroxyl group to the octyl side chain (Fig. 6, Panel D), though the exact arrangement cannot be determined. Daughter ions m/z 113 and m/z 94 indicate that the entire octyl chain and 3-methylpyridine structure, respectively, are intact.

Summary of metabolite structure. Overall our work yields insight into the biodegradation of the three ILs bmpyr, hmpyr, and ompyr through MS and MS/MS analyses. Our work implies that the degradation of bmpyr with its shorter side chain involves unsaturation of the butyl side chain and hydroxylation of the aromatic ring, as opposed to hydroxylation of the side chain as determined by Pham *et al.*[36] This suggests that there are different possible degradation pathways for bmpyr that need to be considered. Our experiments for hmpyr also show unsaturation of the side chain and suggest that degradation by hydroxylation occurs separately on the side chain and on the aromatic ring. Our ompyr results again show degradation by unsaturation of the side chain, as well as hydroxylation of the side chain. While the work of Stotle *et al.*[31] indicates that hydroxylation occurs on the side chain of the IL, this assignment is proposed from MS data alone. Our MS/MS experiments yield daughter ions that are generated solely from the isolated parent ion and strongly suggest hydroxylation to the ring in the case of bmpyr and hmpyr.

These results suggest that fundamentally different biodegradation pathways occur depending on the length of the alkyl chain. These different pathways are inherently linked to the rate of biodegradation, where ompyrBr can be readily degraded through initial hydroxylation of the long octyl chain, but bmpyrBr resists biodegradation because initial hydroxylation occurs on the recalcitrant pyridinium ring instead of the short butyl chain. Our results suggest that different pathways for biodegradation may be applicable depending on the substituted alkyl chain length on the pyridinium ring. Additionally, the differences in our results from those previously published suggest that biodegradation products may exist in different forms, or that degradation may occur at different rates, dependent upon the specific activated sludge microbial community present in the test inoculate. These results provide further evidence that environmental risk assessment of a chemical should take into account several sources of biodegradability information and that molecular microbial community analysis and isolation could yield a proactive means for waste removal.

Toxicity of biodegradation products

While standard biodegradability assays provide useful information concerning the potential activity or persistence of a chemical compound in the environment, and chemical analyses throughout a biodegradation study provide greater insight to the mechanism of catabolism, they do not provide information about how metabolites of the parent pollutant may affect relevant target organisms. Degradation pathways that result in the creation of a compound that is more toxic, capable of bioaccumulation or transport should be carefully avoided in order to fulfill "green chemistry" expectations. For example, microbial biomethylation of mercury creates an organic form that is substantially more lipophilic and toxic to higher organisms.[43] Metabolites of halogenated phenolic compounds containing an *O*-methylation have a significantly higher bioconcentration potential, and are therefore more of an environmental hazard.[44] As mentioned previously, PBDEs can be microbially converted into more toxic debromination products.[11] In light of such cases, it becomes a crucial part of proactive ecotoxicology and green chemistry to understand more about the mechanisms of biodegradability, so that metabolites can be assessed as well as their parent compounds.

In our study, we analyzed toxicity of the biodegradation products over the course of 23 days (for bmpyrBr and hmpyrBr) and 39 days (for ompyrBr) using the standard test organism, *Daphnia magna* (Fig. 7). These tests were performed with mixed microbial cultures enriched from sub-samples taken from the final day of the initial biodegradability experiment instead of with activated sludge communities. While we measured DOC concentrations throughout the experiment, in this case, these measurements were meant only as a guideline for comparison of chemical degradation to toxicity, and not to be used as an OECD-type assessment for ready biodegradability. It should be noted that the timeframe for biodegradation is very different with the enriched cultures than in the original activated sludge community experiment (Fig. 2A *vs.* Fig. 7). For example, bmpyrBr and hmpyrBr degraded fully in 23 days, whereas ompyrBr took 39 days to degrade. This is most likely due to the fact that we did not control for cell density, but rather, transferred enrichments based on volume. While ompyrBr typically degrades more quickly than bmpyrBr and hmpyrBr, cells present in the ompyrBr enrichment culture may have been beyond log-growth phase when the experiment was begun, while bmpyrBr and hmpyrBr cells may have been mid-log phase, accelerating their degradation rates.

We did not see a significant difference in toxicity from the positive control in the bmpyrBr test until Day 23 (Tukey's $p = 0.007$). There was a significant decrease in toxicity through time in the bmpyrBr experimental samples (rmANOVA $p = 0.019$, between subjects). We observed a decrease in toxicity of hmpyrBr on Day 11 (Tukey's $p = 0.053$) and an overall decrease in toxicity through time (rmANOVA $p < 0.001$, between subjects). Finally, there was a significant decrease in toxicity of ompyrBr on Day 39 (Tukey's $p < 0.001$) and a decrease in toxicity through time (rmANOVA $p < 0.001$, between subjects).

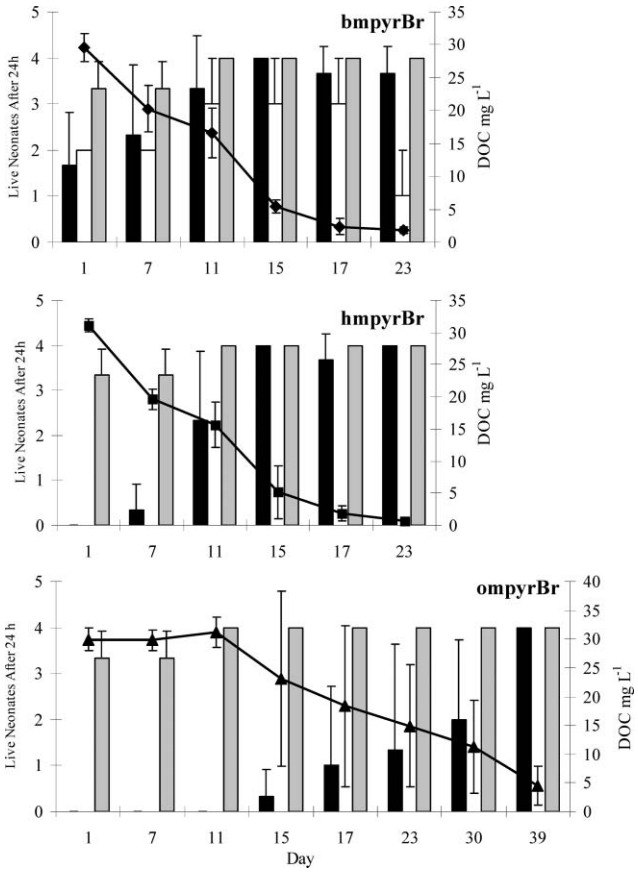

Fig. 7 Number of live *Daphnia magna* neonates after 24 h exposure to biodegradation products (black bars), positive IL control (white bars), negative control with no-IL (gray bars) and DOC concentration in mg L^{-1} (lines) through the experimental time period. Error bars represent ±1 standard deviation ($n = 3$). Positive control treatments killed all *D. magna* in the hmpyrBr and ompyrBr tests, so all values are zero.

In all three tests, there was a strong inverse relationship between DOC concentration and toxicity to *D. magna* ($R^2_{BMP} = 0.862$, $R^2_{HMP} = 0.900$, $R^2_{OMP} = 0.894$). The media with negative controls (no-IL) were consistently nontoxic to *D. magna*, suggesting that the toxic effect is due only to the presence of the IL. At the test concentrations, the hmpyrBr and ompyrBr positive controls were very toxic and above the previously-determined IC-50 values for *D. magna*.[45] Thus, the positive controls for hmpyrBr and ompyrBr tests killed all neonates within the 24 h test period (Fig. 7). In the bmpyrBr tests, fewer neonates died in the positive controls because of the relatively low toxicity of this IL to *D. magna*.[45]

Results of this study suggest that pyridinium-cation ILs can be fully biodegraded and that the metabolites of biodegradation are significantly less toxic to a common aquatic organism. Further, we show that pyridinium-ILs appear to degrade *via* several pathways, potentially depending upon the microbial community acting upon them. Therefore, pyridinium-IL degradation may be more ubiquitous than other potentially more-persistent ILs with imidazolium or quaternary ammonium cations.[31,32,34] Further study is necessary to determine which organisms and enzymes may promote each degradation pathway. Also, while microbial degradation of 1-alkyl-3-methylpyridinium bromide ILs results in non-toxic metabolites, further study is necessary to determine whether metabolites of the more biodegradable ester substituted pyridiniums or ILs with octylsulfate anions are equally non-toxic.[37] Additionally, biotransformation of ILs by plants and animals is still a largely unexamined area of research. While some studies have examined the toxicity of ILs to the cytochrome P450 complex,[46] no studies thus far have shown whether eukaryotic cell conversion of ILs might result in more or less harmful metabolites. A classic example of such an adverse consequence of biotransformation is the conversion of the drug Prontosil by animal cells into a sulfanilamide (antibiotic) compound which competitively blocks the incorporation of 4-aminobenzoate into the vitamin folic acid, thus creating a toxic effect.[9] Few studies to date have sought to examine multiple trophic-level ecotoxicology and biotransformation of ILs, the full effects of which might be masked by standard single-species toxicity tests (see ref. 26–28 for recent exceptions). Additionally, further tests investigating the biodegradability of ILs by natural microbial communities may provide greater insight as to the potential persistence of ILs in the environment.

Experimental

Test compounds

The three pyridinium test compounds used in this study, 1-butyl-3-methylpyridinium bromide (bmpyrBr), 1-hexyl-3-methylpyridinium bromide (hmpyrBr) and 1-octyl-3-methylpyridinium bromide (ompyrBr) (Fig. 1) were synthesized by Dr JaNeille Dixon, University of Notre Dame, Department of Chemical Engineering, using standard procedures.[47–49]

Biodegradability by activated sludge microbial communities

We used a modified OECD Guideline for Testing of Chemicals standard dissolved organic carbon (DOC) Die-Away Test to assess the biodegradability of three pyridinium ILs: bmpyrBr, hmpyrBr and ompyrBr.[39] An activated sludge microbial community sample collected from the South Bend Wastewater Treatment Facility (South Bend, IN, USA) and pre-conditioned by aerating at room temperature for five days. At the end of the aeration period, the total suspended solid concentration (TSS) of the sludge inoculate was determined to be 4.14 g L^{-1}. We prepared three replicate 1-L bottles with sterile mineral medium containing: 0.085 g L^{-1} KH_2PO_4, 0.2175 g L^{-1} K_2HPO_4, 0.334 g L^{-1} $Na_2HPO_4{\cdot}2H_2O$, 5 mg L^{-1} NH_4Cl, 36.4 mg L^{-1} $CaCl_2{\cdot}2H_2O$, 22.5 mg L^{-1} $MgSO_4{\cdot}7H_2O$, 0.25 mg $FeCl_3{\cdot}6H_2O$, as per the OECD guidelines.[39] Each of the three ILs was added to the media at a concentration of 30 mg C L^{-1} for each test. We inoculated the bottles with 7.25 mL of activated sludge sample and diluted each experimental replicate to 1000 mL, to yield a final concentration of 30 mg suspended solids per liter. We inoculated three replicate 1-L bottles containing mineral medium with no-IL as biotic controls. Additionally, we created one replicate bottle for each IL treatment with mineral medium treatment and no bacterial inoculate, to control for abiotic degradation of the ILs.

All 15 treatment and control flasks were shaken aerobically at room temperature during a 41-day incubation period. We

removed 10 mL of sample 23 times (approximately 3 times per week) from the bottles for DOC concentration analysis. The samples were syringe filtered (0.22 μm pore size) and acidified using 100 μL of 2 N HCl. We measured nonpurgeable DOC concentrations within 48 h of collecting the samples by combustion on a Shimadzu TOC5000 with an autosampler. We continued to monitor DOC concentrations until they reached a level below 5 mg L^{-1}, which occurred on Day 26 for ompyrBr and on Day 41 for hmpyrBr and bmpyrBr. After each test, DOC data were analyzed using repeated measures ANOVA (rmANOVA), and then one-way ANOVA with a Tukey's pairwise comparison test at significant time points.

Biodegradation product analysis by reverse-phase HPLC/mass spectrometry

Sub-samples were removed throughout the incubation period for reverse-phase high-performance liquid chromatography/mass spectrometry (RP-HPLC/MS) analysis on Days 1, 10, 17, 24, 29, 35 and 41 (approximately once per week) for the bmpyrBr and hmpyrBr tests and on Days 1, 10, 17, 21, 24, 29 and 33 for the ompyrBr test. Sub-samples (10 mL) were syringe-filtered (0.22-μm pore size) and we measured the total absorbance at 265 nm, corresponding to maximum absorbance of the pyridinium ring, using a Spectronic Genesys 2 spectrophotometer. We then freeze-dried one replicate from each IL treatment for 24 h and rehydrated each in 1 mL of sterile deionized water to yield a 10-fold concentration increase to aid in detecting low concentration products. Methods from Stepnowski *et al.*[50] were used as a starting point for analysis, but optimized for our particular experiment. Samples were analyzed using an Alliance 2690 HPLC system (Waters, Milford, MA) equipped with a 996 photoiodide array detector and interfaced with a Micromass Quattro LC triple quadrupole mass spectrometer (Micromass, Manchester, UK) with an electrospray ionization source operated in the positive-ion mode. This technique enabled both UV and mass spectrometric detection. Absorbance spectra in the HPLC were monitored from 210 to 320 nm, and mass spectra were acquired over the mass range 20 to 600 at a scan rate of 1.5 s. A 10–20 μL sample was injected onto a 4.6 × 150 mm, 3 μm particle size Atlantis dC18 analytical column (Waters) with a 4.6 × 20 mm 3 μm particle size Atlantis dC18 guard column. The mobile phase consisted of (A) 0.5% formic acid in acetonitrile and (B) 20 mM aqueous ammonium acetate. The initial mobile phase for bmpyrBr-based samples was 90% A/10% B (v/v) with a 15 min linear gradient to 40% B (v/v). For hmpyrBr-based samples we used an 80% A/20% B to 60% A/40% B 15-minute linear gradient. For ompyrBr-based samples, we used a 70% A/30% B to 50% A/50% B 15-minute linear gradient. For each method there was an additional 5 min step following the gradient to re-equilibrate the column with the initial mobile phase. The HPLC eluent was split 50 : 50 prior to entering the electrospray ion source of the mass spectrometer. Mass spectrometer scans were conducted in the electrospray positive-ion mode with the following conditions: capillary voltage 3.2 kV, cone voltage 20 V, extraction voltage, 4 V, RF lens 0.2 V, source temperature 150 °C and desolvation temperature 325 °C. We conducted MS/MS experiments using argon as the collision gas and collision energies of 45 kV or 100 kV, and using the same parameters as above except: RF lens 0.4 V, source temperature 125 °C and desolvation temperature 300 °C.

Toxicity of biodegradation products

We created enrichment cultures using 100 mL sub-samples from the final day of the above biodegradation experiment (*i.e.* Day 40 for bmpyrBr and hmpyrBr and Day 33 for ompyrBr) inoculated into 100 mL of fresh IL media, for each respective IL. These mixed cultures were transferred into fresh IL media once every 2 weeks for 6 weeks to maintain an active microbial community, capable of degrading each respective IL. After the third transfer, we inoculated 100 mL of each of the enrichment cultures into 1 L flasks containing 900 mL of fresh, sterile IL media. We did not control for biomass in the inoculations, so different cell numbers may have been inoculated into each set of IL media. Throughout the experimental period, we removed 10 mL sub-samples for DOC analysis as described above to monitor biodegradation progress and 50 mL sub-samples for toxicity analysis. Sampling dates were dependent upon the [DOC] response. For bmpyrBr and hmpyrBr, we removed sub-samples for [DOC] and toxicity analyses on Days 1, 7, 11, 15, 17 and 23. For ompyrBr, we removed sub-samples on Days 1, 7, 11, 15, 17, 23, 30 and 39.

The 50 mL sub-samples used for toxicity testing were filtered through 0.22 μm pore size vacuum filters and then diluted to 100 mL with aerated groundwater in 250 mL acid-washed beakers. Additionally, 3 replicate 50 mL controls of fully concentrated (30 mg C L^{-1}) IL media (positive control) and no-IL media (negative control) were diluted in aerated groundwater as well. We performed 24 h standard acute toxicity tests at each sampling date during the IL experiment until concentrations reached <5 mg C L^{-1}, using *Daphnia magna*, a standard aquatic toxicity test organism. Stock animals were obtained from Carolina Biological Supply (Burlington, NC, USA) and cultured in the lab for several months before use. Cultures were fed Spirulina Dry Powder Microalga (Petaluma, CA, USA) resuspended in groundwater until separation for the toxicity test. For each toxicity test, we used an amended version of the standard *D. magna* acute toxicity test method developed by Sprague[51] and employed by Bernot *et al.*[25] We used four *D. magna* neonates (age <24 h) born from parthenogenic females grown in batch cultures for each experimental unit. The number of living and dead neonates was noted after 24 h exposure, where neonates observed as motionless and without a heartbeat were considered to be dead. The median lethal concentrations (LC-50) of all three ILs to *D. magna* have previously determined to be 13.3 mg L^{-1} bmpyrBr, 1.0 mg L^{-1} hmpyrBr and 0.7 mg L^{-1} ompyrBr.[45]

Positive, negative and control toxicity data were analyzed using repeated measures analysis of variance (rmANOVA). At time points where significant differences occurred, we used a one-way ANOVA and Tukey's HSD pairwise comparison tests. Additionally, we examined regressions between DOC concentration and number of live neonates through time to compare biodegradability to toxicity.

Acknowledgements

We thank Joan Brennecke and JaNeille Dixon for providing ILs, David Costello, Brendan Bohannan and Jessica Bryant for assistance in manuscript preparation, Ken Smdzinski and the City of South Bend, Indiana Wastewater Treatment Facility for assistance in activated sludge sample collection. Thanks to Mike Brueseke for his assistance with *Daphnia* toxicity tests. We also thank Dr Bill Boggess, Dennis Birdsell and the University of Notre Dame Center for Environmental Science and Technology (CEST) for their assistance with HPLC-MS and MS/MS analysis. Funding was provided by the National Science Foundation Graduate Research Fellowship Program, National Oceanic and Atmospheric Administration (Grant #NO04OAR4600076, #NA05OAR4601153), the U.S. Department of Education Graduate Assistance in Areas of National Need (GAANN) Fellowship Program (P200A010448) and the State of Indiana 21st Century Science and Technology Fund (Grant #909010455).

References

1 T. Collins, *Green Chem.*, 2003, **5**, G51–G52.
2 P. T. Anastas and L. M. Warner, *Green Chemistry: Theory and Practice*, Oxford University Press, New York, 1998.
3 M. H. Wake, *BioScience*, 2008, **58**, 349–353.
4 K. J. Kulacki, D. T. Chaloner, D. M. Costello, K. M. Docherty, J. H. Larson, R. J. Bernot, M. A. Brueseke, C. F. Kulpa and G. A. Lamberti, *Chim. Oggi*, 2007, **25**, 32–36.
5 P. J. Van den Brink, *Environ. Sci. Technol.*, 2008, **42**, 8999–9004.
6 K. D. Kimball and S. A. Levin, *BioScience*, 1985, **35**, 165–171.
7 J. Cairns, *BioScience*, 1986, **36**, 670–672.
8 J. Cairns, *Hydrobiologia*, 1983, **100**, 47–57.
9 A. H. Neilson, *Organic Chemicals in the Aquatic Environment: Distribution, Persistence and Toxicity*, CRC Press, Boca Raton, FL, 1994.
10 L. P. Wackett and C. D. Hershberger, *Biocatalysis and Biodegradation: Microbial Transformation of Organic Compounds*, ASM Press, Washington, D.C., 2001.
11 J. Z. He, K. R. Robrock and L. Alvarez-Cohen, *Environ. Sci. Technol.*, 2006, **40**, 4429–4434.
12 *Bioremediation: Applied Microbial Solutions for Real-World Environmental Cleanup*, ed. R. M. Atlas and J. Philip, ASM Press, Washington, D.C., 2005.
13 Y. Song, X. F. Zhu, X. L. Wang and M. J. Wang, *J. Power Sources*, 2006, **157**, 610–615.
14 K. Lundell, T. Kurki, M. Lindroos and L. T. Kanerva, *Adv. Synth. Catal.*, 2005, **347**, 1110–1118.
15 J. L. Bravo, I. Lopez, P. Cintas, G. Silvero and M. J. Arevalo, *Ultrason. Sonochem.*, 2006, **13**, 408–414.
16 K. S. Yeung, M. E. Farkas, Z. L. Qiu and Z. Yang, *Tetrahedron Lett.*, 2002, **43**, 5793–5795.
17 S. V. Malhotra and Y. Xiao, *Aust. J. Chem.*, 2006, **59**, 468–472.
18 W. Pei, J. Mo and J. L. Xiao, *J. Organomet. Chem.*, 2005, **690**, 3546–3551.
19 D. Behar, P. Neta and C. Schultheisz, *J. Phys. Chem. A*, 2002, **106**, 3139–3147.
20 W. Z. Zhang, L. J. He, Y. L. Gu, X. Liu and S. X. Jiang, *Anal. Lett.*, 2003, **36**, 827–838.
21 M. Freemantle, *Chem. Eng. News*, 2005, **83**, 33–38.
22 Y. Zhang, B. R. Bakshi and E. S. Demessie, *Environ. Sci. Technol.*, 2008, **42**, 1724–1730.
23 S. Stolte, J. Arning, U. Bottin-Weber, A. Muller, W. R. Pitner, U. Welz-Biermann, B. Jastorff and J. Ranke, *Green Chem.*, 2007, **9**, 760–767.
24 K. M. Docherty, S. Z. Hebbeler and C. F. Kulpa, *Green Chem.*, 2006, **8**, 560–567.
25 R. J. Bernot, M. A. Brueseke, M. A. Evans-White and G. A. Lamberti, *Environ. Toxicol. Chem.*, 2005, **24**, 87–92.
26 R. J. Bernot, E. E. Kennedy and G. A. Lamberti, *Environ. Toxicol. Chem.*, 2005, **24**, 1759–1765.
27 M. A. Evans-White and G. A. Lamberti, *Environ. Toxicol. Chem.*, 2009, **28**, 418–426.
28 D. M. Costello, L. M. Brown and G. A. Lamberti, *Green Chem.*, 2009, **11**, 548–553.
29 K. M. Docherty, J. K. Dixon and C. F. Kulpa, *Biodegradation*, 2007, **18**, 481–493.
30 M. Stasiewicz, E. Mulkiewicz, R. Tomczak-Wandzel, J. Kumirska, E. M. Siedlecka, M. Golebiowski, J. Gajdus, M. Czerwicka and P. Stepnowski, *Ecotoxicol. Environ. Saf.*, 2008, **71**, 157–165.
31 S. Stolte, S. Abdulkarim, J. Arning, A. K. Blomeyer-Nienstedt, U. Bottin-Weber, M. Matzke, J. Ranke, B. Jastorff and J. Thoming, *Green Chem.*, 2008, **10**, 214–224.
32 A. Romero, A. Santos, J. Tojo and A. Rodriguez, *J. Hazard. Mater.*, 2008, **151**, 268–273.
33 J. R. Harjani, J. Farrell, M. T. Garcia, R. D. Singer and P. J. Scammells, *Green Chem.*, 2009, **11**, 821–829.
34 H. Sutterlin, R. Alexy, A. Coker and K. Kummerer, *Chemosphere*, 2008, **72**, 479–484.
35 J. R. Harjani, R. D. Singer, M. T. Garcia and P. J. Scammells, *Green Chem.*, 2008, **10**, 436–438.
36 T. P. T. Pham, C. W. Cho, C. O. Jeon, Y. J. Chung, M. W. Lee and Y. S. Yun, *Environ. Sci. Technol.*, 2009, **43**, 516–521.
37 J. R. Harjani, R. D. Singer, M. T. Garcia and P. J. Scammells, *Green Chem.*, 2009, **11**, 83–90.
38 P. Stepnowski and P. Storoniak, *Environ. Sci. Pollut. Res.*, 2005, **12**, 199–204.
39 *OECD Guidelines for Testing Chemicals 301 A–F*, Organisation for Economic Co-operation and Development, Paris, France, 1992.
40 C. J. van der Gast, A. S. Whiteley and I. P. Thompson, *Environ. Microbiol.*, 2004, **6**, 254–263.
41 C. J. van der Gast, D. Ager and A. K. Lilley, *Environ. Microbiol.*, 2008, **10**, 1411–1418.
42 M. Manefield, R. I. Griffiths, M. B. Leigh, R. Fisher and A. S. Whiteley, *Environ. Microbiol.*, 2005, **7**, 715–722.
43 S. Jensen and A. Jernelov, *Nature*, 1969, **223**, 753–754.
44 A. S. Allard, M. Remberger and A. H. Neilson, *Appl. Environ. Microbiol.*, 1987, **53**, 839–845.
45 D. J. Couling, R. J. Bernot, K. M. Docherty, J. K. Dixon and E. J. Maginn, *Green Chem.*, 2006, **8**, 82–90.
46 For example: K. L. Tee, D. Roccatano, S. Stolte, J. Arning, J. Bernd and U. Schwaneberg, *Green Chem.*, 2008, **10**, 117–123.
47 P. Bonhote, A. P. Dias, N. Papageorgiou, K. Kalyanasundaram and M. Gratzel, *Inorg. Chem.*, 1996, **35**, 1168–1178.
48 C. M. Gordon, J. D. Holbrey, A. R. Kennedy and K. R. Seddon, *J. Mater. Chem.*, 1998, **8**, 2627–2636.
49 L. Cammarata, S. G. Kazarian, P. A. Salter and T. Welton, *Phys. Chem. Chem. Phys.*, 2001, **3**, 5192–5200.
50 P. Stepnowski, *Aust. J. Chem.*, 2005, **58**, 170–173.
51 J. B. Sprague, *Water Res.*, 1969, **3**, 793–821.

